

Correlations in avalanche critical points

Benedetta Cerruti¹ and Eduard Vives^{1,*}

¹ *Departament d'Estructura i Constituents de la Matèria, Universitat de Barcelona
Martí i Franquès 1, Facultat de Física, 08028 Barcelona, Catalonia*

(Dated: November 13, 2018)

Avalanche dynamics and related power law statistics are ubiquitous in nature, arising in phenomena like earthquakes, forest fires and solar flares. Very interestingly, an analogous behavior is associated with many condensed matter systems, like ferromagnets and martensites. Bearing it in mind, we study the prototypical 3D RFIM at $T = 0$. We find a finite correlation between waiting intervals between avalanches and the previous avalanche size. This correlation is not found in other models for avalanches, such as the standard BTW model, but it is experimentally found in earthquakes and in forest fires. Our study suggests that this effect occurs in critical points which are at the end of an athermal first-order transition line separating two behaviors: one with high activity from another with low activity.

PACS numbers: 05.70.Jk, 05.40.-a, 75.60.Ej,, 75.40.Mg, 75.50.Lk

In the last few years much experimental and theoretical effort has been devoted to the study of avalanche processes. Deep understanding of the statistical correlations in such stochastic processes is needed in order to make advances towards predictability. The importance of the subject is beyond discussion due to the many implications in natural disasters and social crises. Avalanche processes are characterized by extremely fast events whose occurrences are separated by waiting intervals without activity. The magnitudes characterizing avalanches (energy, size, duration) are, in most cases, statistically distributed according to a power law $p(s)ds \sim s^{-\tau}ds$ characterized by a critical exponent τ : extremely large events hardly occur, whereas small events are very common. This is the famous Gutenberg-Richter law for earthquakes. Power-law distributions have been found not only for other large-scale natural phenomena ranging from solar flares [1] to forest-fires [3], but also in laboratories associated with many condensed matter systems: condensation [2], ferromagnets [4], martensitic transitions [5], superconductivity [6], etc. However, statistics of waiting intervals δ are not often studied, especially in condensed matter. The distribution $p(\delta)d\delta$ has been described by different laws including exponentials and also power-laws. For solar flare statistics and earthquake models, it has been found [7, 8] that the unavoidable threshold definition (separating activity from inactivity) alters the distribution $p(\delta)$ and that this thresholding effect is a signature of the existence of correlations [9, 10]. Direct measurement of the correlations between waiting intervals and avalanche sizes has been obtained by measuring the constrained interval distributions $p_{prev}(\delta|s > s_0)$ and $p_{next}(\delta|s' > s_0)$. These are the probabilities of having a waiting interval δ , given that the previous (s) or the next (s') avalanche is larger than s_0 . For earthquake and forest-fire statistics, while p_{next} has been found to be independent of s_0 , p_{prev} does exhibit significant changes when varying s_0 [11, 12].

In this letter we study some statistical correlations for the 3D-RFIM at $T = 0$ with metastable dynamics based on the local relaxation of single spins. This model was introduced [13] for the study of Barkhausen noise in ferromagnets [4] and acoustic emission in martensitic transitions [5], and has been used as a prototype for the study of crackling noise and other avalanche phenomena [14, 15]. The model is defined on a cubic lattice with size $N = L^3$. At each lattice site there is a spin variable $S_i = \pm 1$ ($i = 1, \dots, N$) that interacts with its nearest neighbors (n.n.) according to the Hamiltonian (magnetic enthalpy):

$$\mathcal{H} = - \sum_{n.n.} S_i S_j - \sum_{i=1}^N S_i h_i - H \sum_{i=1}^N S_i. \quad (1)$$

The local random fields h_i are Gaussian distributed with zero mean and standard deviation σ . This parameter not only allows the critical behavior ($\sigma = \sigma_c \simeq 2.21 \pm 0.01$) to be studied but also subcritical ($\sigma > \sigma_c$), and supercritical ($\sigma < \sigma_c$) regimes [16, 17]. This tuning is absent in so-called Self-Organized Criticality models like the original BTW model [18], in which the critical state is reached after waiting for a certain time without any parameter adjustment. In the RFIM, the time variable is replaced by the external field H , which is adiabatically increased from $-\infty$ to ∞ . The system responds by an increase of the order parameter $m \equiv \sum_{i=1}^N S_i / N$ (magnetization per spin) from -1 to 1 . The spins flip according to the dynamical rule $S_i = \text{sign}(\sum_j S_j + h_i + H)$ (the first sum runs over the n.n. of spin S_i), which corresponds to a minimization of the local energy. This non-equilibrium dynamics leads to hysteresis and avalanches when many spins flip at constant field. The avalanche size s is defined as the number of spins flipped until a new stable state is reached. Avalanches are separated by field waiting intervals δ without activity. When $\sigma = \sigma_c$ and H is close to $H_c \simeq 1.43 \pm 0.05$ [16, 19], the avalanche size distribution becomes approximately a power law $p(s) \sim s^{-\tau}$

(with $\tau \simeq 1.6$ [16]). The properties of large (percolating) avalanches at the critical point have been previously discussed [19]. Critical avalanches have been found to be fractal so that $\langle s \rangle_c \sim L^{d_f}$ with $d_f \sim 2.88$. When $\sigma > \sigma_c$, the avalanche distribution is exponentially damped, i.e. all avalanches are negligible compared to system size, and the magnetization m evolves continuously when the system is infinite. For $\sigma < \sigma_c$, avalanches are also infinitesimally small compared to L^3 , except for a unique infinitely large and compact ($s \sim L^3$) avalanche corresponding to a first-order phase transition between a phase with low m and a phase with high m . The first-order transition line can be linearly approximated by the equation $H_t(\sigma) = H_c [1 - B'(\sigma - \sigma_c)/\sigma_c]$ with $B' = 0.25$. [19]

In this letter we will concentrate on the analysis of the field waiting intervals δ , and their correlation with the previous and next avalanche sizes. We have first checked that intervals are exponentially distributed. Fig. 1 shows the distribution of waiting intervals for $\sigma = 2.21$, $L = 30$ and three different H -ranges. One can observe that before and after the transition region the distributions are very well described by exponentials (continuous lines), whereas in the transition region the distribution becomes a linear mixture of exponentials. The mean value $\langle \delta \rangle$, which is the only parameter characterizing such distributions, depends on σ and H , and below σ_c it exhibits a discontinuity $\Delta \delta$ when H increases and crosses the first-order transition line from the region of high activity (small $\langle \delta \rangle$) to the region of low activity (large $\langle \delta \rangle$), as shown in the inset of Fig. 1. We can, therefore, compare the behavior of the discontinuity $\Delta \delta$ to that of an order parameter. Note that, given the finite size of the system, the pseudo-critical point where the mixture of exponentials becomes a single exponential distribution will be located at $\sigma > 2.21$. For this reason, although data in Fig. 1 correspond to σ_c , one can still observe a range of fields with the two-peak distribution.

Besides the histogram analysis, we have numerically checked that for all σ and H , $\langle \delta \rangle \sim \sqrt{\langle \delta^2 \rangle - \langle \delta \rangle^2}$, [20] which is more evidence of the exponential character of $p(\delta)$. The continuous line in the inset of Fig. 1 shows this agreement, except for some deviations close to the transition line due to finite-size effects.

For the following discussions it is interesting to analyze the finite-size dependence of $\langle \delta \rangle$. A simple argument can be used to state that far from the critical point, since the correlation length is finite, the probability for an avalanche to start when the field is increased by dH is proportional to the number of triggering sites and thus to L^3 . This implies that $\langle \delta \rangle \sim L^{-3}$. Fig. 2 shows examples of this behavior for different values of σ and H . At criticality, the correlation length diverges and the triggering argument may be too naive. Nevertheless, as shown in Fig. 2, numerical simulations indicate that the exponent is always very close to 3. Uncertainties in H_c and σ_c do not allow for an accurate enough finite-size scaling anal-

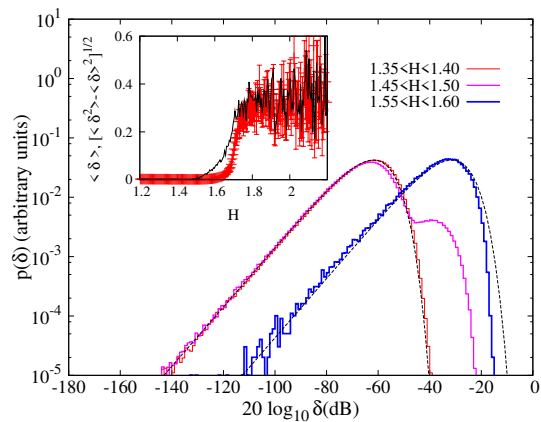


FIG. 1: Log-log plot of the histograms corresponding to the distribution of waiting intervals δ for $L = 30$, $\sigma = 2.21$ and three different field ranges, indicated by the legend. Note that the horizontal scale is in dB and bins are logarithmic. The dashed lines show fits corresponding to the exact exponential behavior. Data have been obtained by averaging over 50000 realizations of disorder. The inset shows the behavior of $\langle \delta \rangle$ (symbols) and $\sqrt{\langle \delta^2 \rangle - \langle \delta \rangle^2}$ (continuous line) as a function of H for $\sigma = 1.95$ and $L = 30$.

ysis to determine small variations. For the discussions here the exact value of this exponent is not needed and we will assume that $\langle \delta \rangle \sim L^{-z}$ with $z \sim 3$.

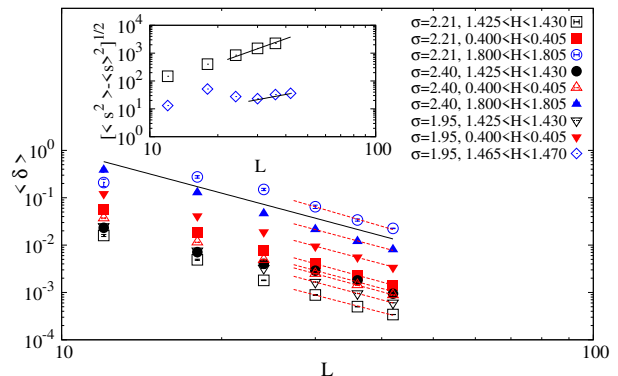


FIG. 2: Log-log plot of the average waiting interval $\langle \delta \rangle$ as a function of the system size L for different values of σ and H as indicated by the legend. The continuous line shows the behavior L^{-3} and the discontinuous lines are fits to the last 2-3 points for each series of data. Data are averaged over 50000 disorder realizations. The inset shows the behavior of $\sqrt{\langle s^2 \rangle - \langle s \rangle^2}$ for the values of σ and H indicated. The continuous lines show the behavior L^{d_f} (above) and $L^{3/2}$ (below).

Let us now focus on the study of correlations and consider a sequence of two avalanches, the first with size s , then a waiting interval δ , and the next avalanche with

size s' . We define the following two correlation functions:

$$\rho_{s,\delta} = \frac{\langle s\delta \rangle - \langle s \rangle \langle \delta \rangle}{\sqrt{\langle s^2 \rangle - \langle s \rangle^2} \sqrt{\langle \delta^2 \rangle - \langle \delta \rangle^2}} \quad (2)$$

$$\rho_{\delta,s'} = \frac{\langle s'\delta \rangle - \langle s' \rangle \langle \delta \rangle}{\sqrt{\langle s'^2 \rangle - \langle s' \rangle^2} \sqrt{\langle \delta^2 \rangle - \langle \delta \rangle^2}} \quad (3)$$

Fig. 3 shows examples of the behavior of the correlation functions for different system sizes and $\sigma = \sigma_c \simeq 2.21$ as a function of the scaling variable $v = [(H - H_c)/H_c] L^{1/\mu}$ that measures the distance to the critical point. The exponent $\mu = 1.5$ has been taken from the literature [19]. (Note that this scaling variable only takes three values in the thermodynamic limit $v = \pm\infty, 0$).

For the understanding of the behavior of the correlation functions for increasing system size, one must first discuss what the expected behavior of a generic correlation function $\rho(H, \sigma = \sigma_c, L)$ close to H_c is likely to be. It should be borne in mind that correlations are, by definition, bounded between -1 and 1 . Therefore no critical divergences can occur with increasing L . Consequently, any critical correlation either goes to zero or tends to a constant value. In this second case, it should exhibit scaling behavior $\rho(H, \sigma_c, L) \sim \hat{\rho}(\sigma_c, v)$.

The first observation from Fig. 3 is that $\rho_{\delta,s'}$ is much smaller than $\rho_{s,\delta}$ not only at the critical point ($v = 0$), but also for other values of the field. In addition, the data shows that $\rho_{\delta,s'}$ systematically decreases in absolute value with increasing system size. Therefore the numerical data is consistent with a vanishing $\rho_{\delta,s'}$ in the thermodynamic limit.

The second important observation is that correlation between an avalanche size and the next waiting time, $\rho_{s,\delta}$ exhibits a constant value ~ 0.4 at the critical point. The overlap of the curves is rather good, specially if one takes into account the fact that even at the critical point there are non-critical avalanches which may slightly perturb the scaling function behavior. The fact that the scaling function in Fig. 3(a) goes to zero for $v \rightarrow \pm\infty$ indicates that the finite correlation only survives exactly at the critical point, but vanishes for fields both above and below. We would like to note that the result of a finite correlation $\rho_{s,\delta}$ is not in contradiction with the Poissonian character for the triggering instants of the avalanches.

A second way to go deeper into the understanding of the nature of the correlations is the direct measurement of the restricted distribution of intervals $p_{prev}(\delta|s > s_o)$ and $p_{next}(\delta|s' > s_o)$. Fig. 4 shows, as an example, the dependence of these two distributions for $L = 30$, $\sigma = 2.21$ and $1.40 < H < 1.45$. The distribution of intervals $p_{prev}(\delta|s > s_o)$ clearly exhibits a dependence on the previous avalanche size, whereas $p_{next}(\delta|s' > s_o)$ is independent of s_o . Thus, the larger the size of an avalanche, the larger the probability that the following waiting interval is large. We should note at this point that a similar same causal dependence has been found for the statis-

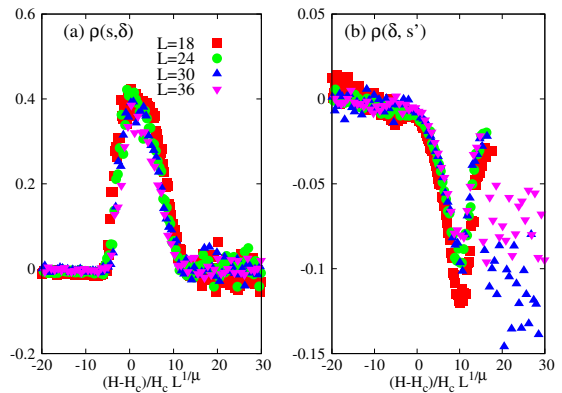


FIG. 3: Correlation functions defined by Eq. (2) and (3) as functions of the scaling variable for $\sigma = 2.21$ and different system sizes as indicated by the legend. Data correspond to averages over 50000 disorder realizations and field intervals with size $\Delta H = 0.005$. Note the different vertical scale in the two figures.

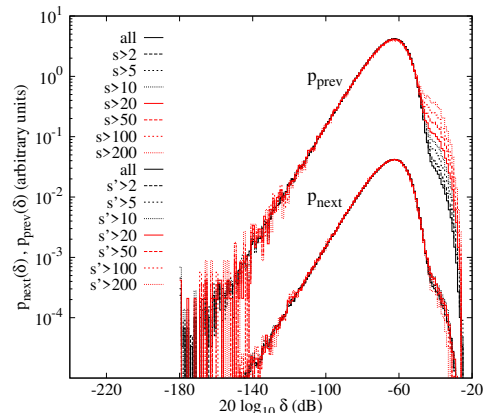


FIG. 4: Log-log plot of the restricted distribution of intervals δ given that the previous (next) avalanche is larger than s_o . p_{prev} has been displaced two decades up in order to clarify the picture.

tics of earthquakes and forest fires [11, 12], but with a different sign. The larger the size of an earthquake, the smaller the waiting time to the next event.

The origin of such correlations in our RFIM can be understood by noting that, for a finite system below σ_c , after an avalanche with a large size (of the order L^3), one can “guess” that the system has jumped to the low-activity region and, therefore, one can “predict” that the next interval δ will be large. We can provide an heuristic argument of why such finite-size correlations vanish in the thermodynamic limit, everywhere except at the critical point. Let us analyze the behavior of the numerator and the two square roots in the denominator in Eq. 2. First note that, given the fact that $p(\delta)$ is exponential, the fluctuations of $\sqrt{\langle \delta^2 \rangle - \langle \delta \rangle^2}$ behave as

$\delta \sim L^{-z}$. The fluctuations of s behave differently below σ_c and at σ_c . If we consider an interval ΔH that crosses the first-order transition region, below σ_c we will have a number of avalanches proportional to L^3 contributing to the averages. Among these, most will display a small size $\sim L^0$ but one will have a size $\sim L^3$. When computing $\langle s \rangle$ we get a $\langle s \rangle \sim L^0$ behavior, but when computing $\sqrt{\langle s^2 \rangle - \langle s \rangle^2}$ we will get $L^{3/2}$, as shown in the inset of Fig. 2 for $\sigma = 1.95$ and the interval $1.465 < H < 1.470$ crossing the transition line. Exactly at criticality, the distribution of avalanches becomes a power-law. This means that the averages $\langle s \rangle$ and $\langle s^2 \rangle$ should be computed by integrating the distribution from 1 to the largest avalanche size which has a fractal dimension $s_{max} \sim L^{d_f}$ [19]. By integration, one trivially gets $\langle s \rangle \sim L^{d_f}$ and $\langle s^2 \rangle \sim L^{2d_f}$. The fluctuations therefore will go as $\sqrt{\langle s^2 \rangle - \langle s \rangle^2} \simeq L^{d_f}$, as shown in the inset of Fig. 2.

To study the numerator in Eq. (2) one should note that $\langle s\delta \rangle - \langle s \rangle \langle \delta \rangle = \langle s'\delta' \rangle - \langle s' \rangle \langle \delta \rangle = \langle s'(\delta' - \delta) \rangle$. This average measures the avalanches that carry an associated change in δ . For $\sigma < \sigma_c$, among the set of L^3 avalanches in an interval ΔH , there is one avalanche with size L^3 associated with a change $\Delta\delta \sim L^{-z}$. The rest of the avalanches have a size L^0 and carry no change in δ . Therefore the numerator in Eq. 2 goes as L^{-z} and consequently, below σ_c , $\rho(s, \delta) \sim L^{-z}/(L^{3/2}L^{-z}) \sim L^{-3/2} \rightarrow 0$.

For $\sigma = \sigma_c$ the behavior of the numerator in (2) is much more intricate since different kinds of critical avalanches exist close to the critical point. Apart from a number of non-critical avalanches, there is an infinite number ($\sim L^\theta$) of spanning avalanches and another infinite number $\sim L^{\theta_{nsc}}$ of critical non-spanning avalanches. It is difficult to argue which of these avalanches have an associated $\Delta\delta$. We cannot provide a definite argument, but, at least, the product $\langle s \rangle \langle \delta \rangle$ (appearing in the numerator of Eq.2) behaves as $L^{d_f}L^{-z}$. Therefore it is plausible that at σ_c , $\rho(s, \delta) \sim L^{d_f-z}/(L^{d_f}L^{-z}) \sim 1$, which justifies the finite value of the correlation $\rho(s, \delta)$ found numerically, as shown in Fig. 3.

In order to compare with the avalanche models based on SOC, we have performed an analysis of the same probability densities and correlations for the 2D-BTW model. In this case, the waiting times are discrete since they are identified with the number of grains added before a new avalanche starts. For large enough systems, these waiting intervals are distributed according to the geometric distribution which is the discrete version of the exponential distribution and all the two correlation functions (2) and (3) clearly vanish.

In summary, we have numerically studied the $T = 0$ RFIM with metastable dynamics as a prototype for avalanche processes in condensed matter systems which display an underlying first-order phase transition. The sequence of avalanches and waiting times can be considered as a compound Poisson process since waiting in-

tervals tend to be exponentially distributed. Nevertheless, correlations between the avalanche size and the next waiting time exist at the critical point in the thermodynamic limit. Such a causal correlation $\rho(s, \delta) \neq 0$ has been found experimentally in earthquakes and forest fires, although with a different sign. This difference could easily be explained by considering a discontinuity $\Delta\delta < 0$. An experimental challenge for the future is to look for these effects in laboratory experiments on condensed matter systems exhibiting avalanches (Barkhausen noise, acoustic emission in martensites, etc).

This work has received financial support from CICYT (Spain), project MAT2007-61200, CIRIT (Catalonia), project 2005SGR00969, B.C. acknowledges the hospitality of ECM Department (Universitat de Barcelona) and a grant from Fondazione A. Della Riccia. We also acknowledge fruitful discussions with A.Corrall, J. Vives and A. Planes.

* Electronic address: eduard@ecm.ub.es

- [1] E.T.Lu, Phys. Rev. Lett. **74**, 2511 (1995); G.Boffetta *et al*, Phys. Rev. Lett. **83**, 4662 (1999).
- [2] M.P.Lilly, P.T.Finley, and R.B.Hallock, Phys. Rev. Lett. **71**, 4186 (1993)
- [3] B.D.Malamud, G.Morein, and D.L.Turcotte, Science **281**, 1840 (1998).
- [4] G.Bertotti, *Hysteresis in magnetism*, Electromagnetism series (Academic Press, Sand Diego, 1998).
- [5] E. Vives *et al*, Phys. Rev. Lett. **72**, 1694 (1994).
- [6] W.Wu and P.W.Adams, Phys. Rev. Lett **74**, 610 (1995).
- [7] D. R.Sánchez and B.A.Carreras, Phys. Rev. Lett. **88**, 068302 (2002).
- [8] M.Paczuski, S.Boettcher, and M.Baiesi, Phys. Rev. Lett. **95**, 181102 (2005).
- [9] R.Woodard, D.E.Newman, R.Sánchez, and B.A.Carreras, Phys. Rev. Lett **93**, 249801 (2004).
- [10] X.Yang, S.Du, and J.Ma, Phys. Rev. Lett **92**, 228501 (2004)
- [11] A.Corrall, L.Telesca, and R.Lasaponara, Phys. Rev. E **77**, 016101 (2008).
- [12] A.Corrall, Phys. Rev. Lett. **95**, 159801 (2005).
- [13] J. P. Sethna *et al*, Phys. Rev. Lett. **70**, 3347 (1993).
- [14] J.P.Sethna *et al*, Nature **410**, 242 (2001).
- [15] F.Detcheverry, E.Kierlik, M.L.Rosinberg, and G.Tarjus, Phys. Rev. E **72**, 051506 (2005).
- [16] O. Perković K. A. Dahmen, and J.P.Sethna, Phys. Rev. B **59**, 6106 (1999).
- [17] F.J.Pérez-Reche and E.Vives, Phys. Rev. B **67**, 134421 (2003).
- [18] P.Bak, C.Tang, and K.Wiesenfeld, Phys. Rev. Lett. **59**, 381 (1987); P.Bak, C.Tang, and K.Wiesenfeld, Phys. Rev. A **38**, 364 (1988).
- [19] F.J.Pérez-Reche and E.Vives, Phys. Rev. B **70**, 214422 (2004).
- [20] Except on the transition line where we expect $\sqrt{\langle \delta^2 \rangle - \langle \delta \rangle^2} \sim \sqrt{\langle \delta \rangle^2 - k_0 \Delta \delta^2}$ with $k_0 = \text{constant}$.